Novel Self–Assembly of Amphiphilic Copolymers into Nanotubes: Characterization by Small–Angle Neutron Scattering †

5 AUTHORS, INCLUDING:

Terence Cosgrove
University of Bristol
245 PUBLICATIONS **5,436** CITATIONS

SEE PROFILE

Robert M Richardson
University of Bristol
194 PUBLICATIONS **3,350** CITATIONS

SEE PROFILE

Michael Whitehead
McGill University
223 PUBLICATIONS **2,336** CITATIONS

SEE PROFILE

Novel Self-Assembly of Amphiphilic Copolymers into Nanotubes: Characterization by Small-Angle Neutron Scattering[†]

C. Malardier-Jugroot,[‡] T. G. M. van de Ven,[*,‡] T. Cosgrove,[§]
R. M. Richardson,[‖] and M. A. Whitehead[‡]

*Department of Chemistry, McGill University, Montreal, Canada, and Departments of
Chemistry and Physics, University of Bristol, Bristol, England*

Received April 4, 2005. In Final Form: August 29, 2005

The self-assembly into nanotubes in solution of an amphiphilic copolymer is characterized by small-angle neutron scattering (SANS). This study confirmed the shape and the size of the tubular association and the 3-D association of the tubes predicted by molecular orbital theory. Moreover, the characterization of the stability of the association has revealed that the addition of a very small amount of salt to the solution increases the size of the association. When more salt is added, the size of the association decreases, and the structure is altered. The association was found to be independent of temperature and therefore is very stable.

The study of block copolymers using neutron scattering has allowed the characterization of different phase separations and conformations of polymer chains in different solvents. The applications of block copolymers are very broad and range from foam stability[1] to drug delivery and nanotechnology.[2] In comparison, the association among alternating copolymer chains has not been widely studied.

In this article, the association of poly(styrene-*alt*-maleic anhydride) (SMA) is investigated. In a previous study, the conformation of SMA chains was determined with theoretical methods at different pH values.[3] The conformation obtained at pH 7 showed a linear structure, regardless of the chirality of the chain, which allows a strong association at pH 7. However at pH 3 and 12, the dependence of the chain conformation on the chirality prevents the association. In a companion paper, the association between the polymer chains was characterized, and the most stable structure obtained in water was found to be a square tubular structure.[4] This tube has an inner radius of 14.0 Å and an outer radius of 20.5 Å. The tubes were shown to associate into sheet, and the sheets can then stack upon each other at an angle of 45° (Figure 1). The theoretical study predicted that the internal surface of the tube is mainly hydrophobic whereas the external surface is mainly hydrophilic. The external size of the tubes as well as their association into sheets and the packing of the sheets was confirmed by cryo-TEM.[4] This neutron-scattering study allows the characterization of the internal and external structure of the tubes and their association in solution. The parameters obtained from this experiment will be compared to the theoretical prediction.

Small-angle neutron scattering (SANS) is a key technique for the study of complex fluids and polymers. This method provides detailed information on the shape and size of polymers as well as on their intermolecular interactions and thermal stability.[5] Neutron-scattering experiments have been widely used to determine the different shapes associated with the phase separation of block copolymer solutions.[6–8]

The main field of application of the SANS technique is the determination of the molecular size and shape in crowded environments. In addition, the conformation of complex systems can be determined by fitting a model form factor $P(Q)$ to the experimental data. Therefore, this technique can be used to characterize in detail the different ordered forms of copolymers.[6] To study the association of SMA at different pH values, two series of neutron-scattering experiments have been performed: one at ILL (Grenoble, France) and the other at NIST (Gaithersburg, MD) facilities.

Selection of a Model

The exact configuration of the interactions between molecules cannot be obtained directly from the scattering intensity curve; therefore, models of the form factor $P(Q)$ for different associations have to be defined to determine the shape and size of the studied system. These form factors have several parameters that can be optimized to fit the experimental intensity curve. These parameters are characteristic of the studied system, for example, the radius of the micelles, the local volume fraction of the association, and so forth. It is therefore important to select a model that is physically reasonable and is capable of fitting the data. The parameters may then be estimated by optimizing the fit using least squares. Hence, the definition of a good model is essential.

The experiments were done in D_2O using hydrogenated SMA (Table 1) to maximize the contrast between the

[†] Part of the Bob Rowell Festschrift special issue.

[‡] McGill University.

[§] Department of Chemistry, University of Bristol.

[‖] Department of Physics, University of Bristol.

(1) Calleja, F.; Roslaniec, Z. *Block Copolymers*; Dekker: New York, 2000.

(2) Zhang, J.; Wang, Z.-L.; Liu, J.; Chen, S.; Liu, G.-Y. *Self-Assembled Nanostructures*; Kluwer Academic/Plenum Publishers: New York, 2003.

(3) Malardier-Jugroot, C.; van de Ven, T. G. M.; Whitehead, M. A. *J. Phys. Chem. A,* submitted for publication, 2004.

(4) Malardier-Jugroot, C.; van de Ven, T. G. M.; Whitehead, M. A. *Nanotechnology,* to be submitted for publication.

(5) Mortensen, K. *Amphiphilic Block Copolymers*; Elsevier Science: The Netherlands, 2000.

(6) Hanson, E.; Borsali, R.; Pecora, R. *Macromolecules* **2001**, *34*, 2208.

(7) Nakano, M.; Matsuoka, H.; Yamaoka, H.; Poppe, A.; Richter, D. *Macromolecules* **1999**, *32*, 697.

(8) Yoshida, K.; Misawa, M.; Maruyama, K.; Imai, M.; Furusaka, M. *J. Chem. Phys.* **2000**, *113*, 2343.
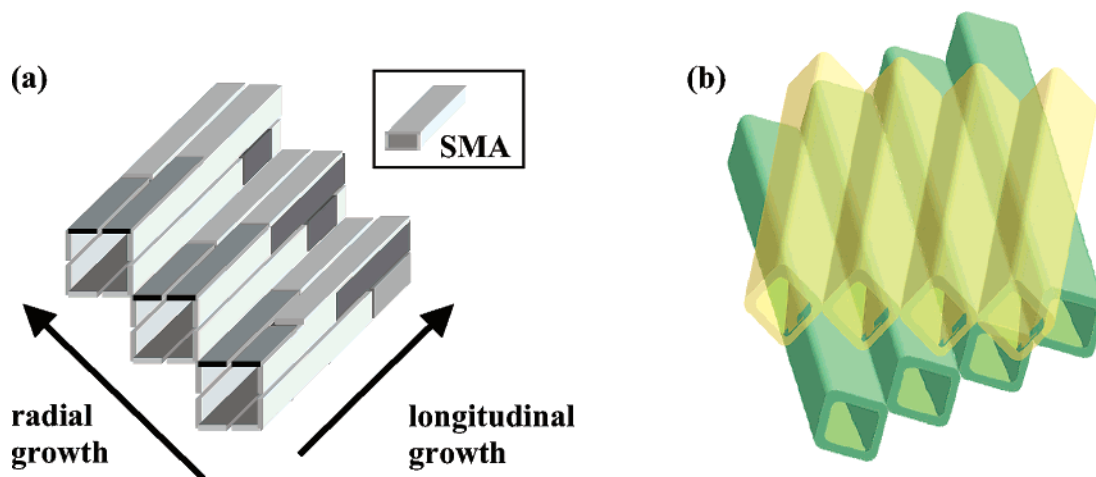
Figure 1. Schematic representation of the association of SMA tubes into sheets (a) and of the packing of sheets into stack of sheets (b).

Table 1. Structure and Scattering-Length Density (SLD) of SMA and D₂O

	SMA	*Solvent*
Structure		
SLD (*10⁻⁵Å⁻²)	0.187	0.638

solvent and the polymer. The scattering curve corresponds to the SMA structure, SMA−SMA association, and intertubular interactions. The scattering-length density (SLD) contrast is caused by the D₂O−SMA scattering-length contrast (Table 1).

The scattering profile obtained for a 1 wt % solution at pH 7 is shown in Figure 2. This profile shows a peak, which is indicative of interacting molecules forming ordered systems.[5] In addition, an increase in intensity at low Q values is observed, indicative of large interactions between these systems.

Using our prior knowledge of the structure of SMA chains' association in solution obtained from the theoretical studies,[4] a model was developed. This model uses the form factor for cylinders:[9,10]

$$P(Q) = \int_0^{\pi/2} \left[\frac{2B_1(QR \sin \alpha)}{QR \sin \alpha} \frac{\sin(QL \cos \alpha)/2}{QL \cos(\alpha/2)} \right]^2 \sin \alpha \, d\alpha \quad (1)$$

In this equation, $B_1(x)$ is the first-order Bessel function; R is the radius and L is the length of the cylinder.

To define a hollow cylinder, the form factors of two coaxial cylinders were combined. The first cylinder represents the shell of the tube and will have the scattering length of the polymer studied. The second cylinder represents the solvent inside the hollow cylinder and will have the scattering length of the solvent. The model is schematized in Figure 3.

$$P(Q) = \left(\frac{1}{R_e^2 - R_i^2} \right)^2 \int_0^{\pi/2} \left[\left(\frac{2B_1(QR_e \sin \alpha)}{QR_e \sin \alpha} - \frac{2B_1(QR_i \sin \alpha)}{QR_i \sin \alpha} \right) \frac{\sin(QL \cos \alpha)/2}{QL \cos(\alpha/2)} \right]^2 \sin \alpha \, d\alpha$$

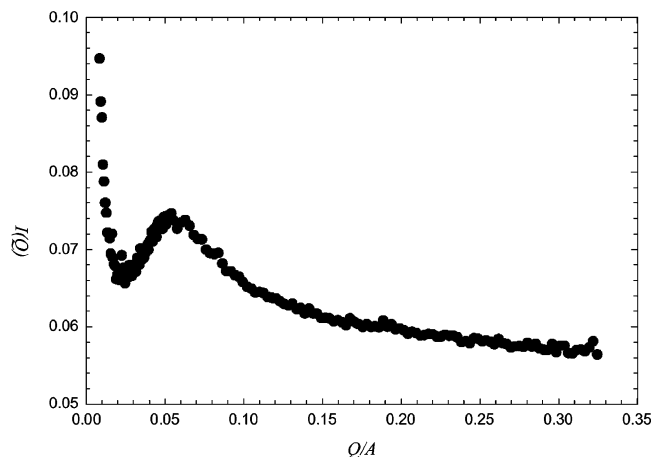where R_e and R_i are as shown in Figure 3.

Figure 2. Neutron-scattering profile of a 1 wt % SMA solution in D₂O at pH 7.

It has been shown from the theoretical calculations as well as from the experimental characterization[4] that the tubes formed by SMA chains are not freely suspended. The increase in the scattering intensity obtained for SMA at low Q (Figure 2) is consistent with the interactions shown schematically in Figure 1. For simplicity, the interaction between two hollow cylinders is modeled using a classical isotropic interaction energy V of the form $V(r) = Ae^{-\kappa r}$ (Figure 3). The function will reflect the combined effect of the form factor of the cylinder and the intercylinder interference function.

This model is not an exact representation of the interaction predicted by the theoretical calculation and

(9) Guinier, A.; Fournet, G. *Small-Angle Scattering of X-ray*; Wiley & Sons: New York, 1955.
(10) Vaia, R.; Krishnamoorti, R.; Benner, C.; Trimer, M. *J. Polym. Sci., Part B: Polym. Phys.* **1998**, *36*, 2449.
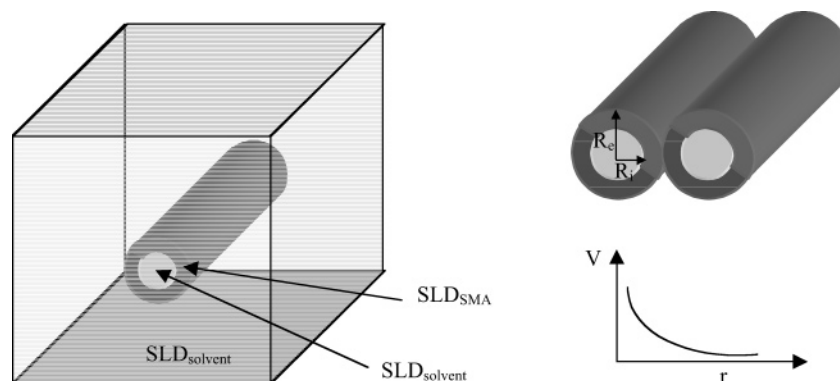
Figure 3. Schematic representation of the interacting hollow cylinders model (SLD$_{solvent}$ is the scattering-length density of the solvent that is used in the internal cylinder in the model of the tube). Potential used to model the interaction between the tubes.
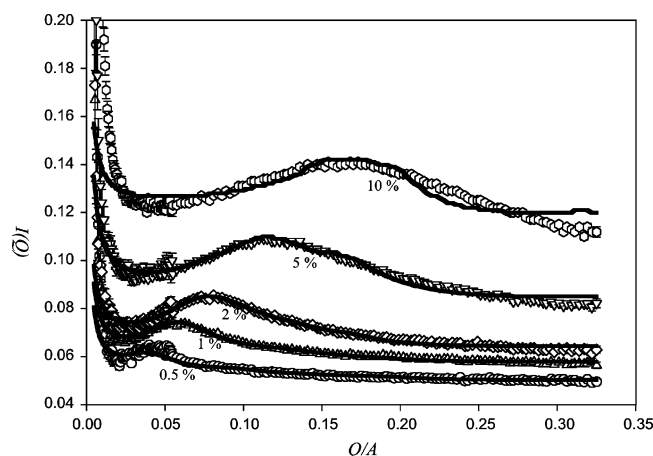

Figure 4. Neutron-scattering profile of different concentrations of SMA in D$_2$O (circles and error bars) fitted by a model of interacting hollow cylinders (line) at pH 7.

observed by cryo-TEM, as indeed it neglects the effect of the packing of the sheets upon each other (Figure 1) and one might expect deviation from the experimental curve for large-scale interactions.

Two other models were used to determine the validity of the hollow cylinder model with interaction: a simple spherical model and a hollow cylinder model without interaction. The two models gave a poor fit even at low concentration.

Concentration Dependence

We first performed SANS experiments on SMA solutions of various concentrations. The results are shown in Figure 4. The solutions in this section were prepared with poly-(styrene−maleic anhydride) (SMA) of molecular weight $M_w = 4 \times 10^4$. The interacting hollow cylinder model described above was used for all of the curve fittings performed in this article. The best fits for the different concentrations are shown in Figure 4.

Several parameters used to fit the experimental curves were known and therefore fixed during the optimization of the unknown parameters. The fixed parameters were the calculated SLD of the solvent and of the polymer and the total volume fraction. The theoretical inner and outer radii were used as starting points for the optimization of the model form factor but were not fixed during the optimization of the parameters.

The fit corresponds to the continuous lines, and the experimental data correspond to the circles and error bars. This fit shows very close agreement with the experimental curve. For instance, for the 1 wt % solution, the same

Table 2. Theoretical Inner and Outer Radii of the SMA Tube Compared to the Inner and Outer Radii Predicted by the Hollow Cylinder Model

	inner radius (Å)		outer radius (Å)	
	theory	experiment	theory	experiment
0.5 wt %	14.0	13.0 ± 0.8	20.5	19.9 ± 1.5
1 wt %	14.0	12.8 ± 0.6	20.5	19.7 ± 1.2
2 wt %	14.0	12.8 ± 0.6	20.5	22.3 ± 0.7
5 wt %	14.0	12.7 ± 0.7	20.5	22.3 ± 0.7
10 wt %	14.0	12.0 ± 1.4	20.5	21.9 ± 1.0

peak was observed for $Q \approx 0.06$ Å^{-1}, and an increase at low Q values is also predicted by the model. The fit obtained with this model is good, but a discrepancy can be observed at low Q values. This discrepancy is even more pronounced for concentrated solutions and might be caused by the neglect of the packing between the sheets. In addition, the fit obtained for the 10 wt % SMA solution also shows a discrepancy at high Q values.

To confirm the size of the internal and external diameters of the nanotubes in solution, the change in the χ^2 parameter (representing the quality of the fitting) as a function of the internal radius was studied for the 2 wt % solution, which represents an intermediate value. Figure 5a shows the variation of this parameter as a function of the internal radius keeping the difference between the inner and outer radii fixed at 6.5 Å (which is the value predicted by theory). This curve shows a minimum in the χ^2 parameter for an internal radius of 14 Å and an outer radius of 20.5 Å, which correspond to the values predicted theoretically. Figure 5b represents the fits associated with the change in internal radius for a 2 wt % SMA solution.

The internal and external radii found during the optimization of the parameters of the model form factor are very close to the theoretical predictions (Table 2). For the 1 wt % SMA solution, the external radius found by this method (19.7 Å) is in better agreement with theory (20.5 Å) than the external radius found by cryo-TEM (25.0 Å). The good agreement of the fit using the hollow cylinder model experimentally confirms the presence of nanotubes in solution, which were predicted by theory. In addition, the main parameters changing from one concentration to the other are the total and local volume fractions.

The best fit for parameters A and $1/\kappa$ in interaction energy V, which determines the structure factor, is shown in Figure 6. Here, parameter A was fixed because it depends on the charge density of the nanotubes, which is fixed by the chemical structure. Only the Debye length was varied to obtain the best fit. It was found that the best fit data for $1/\kappa$ scale as $1/c^{1/2}$, which is expected because only counterions are present and thus the salt concentration is proportional to the SMA concentration. The data
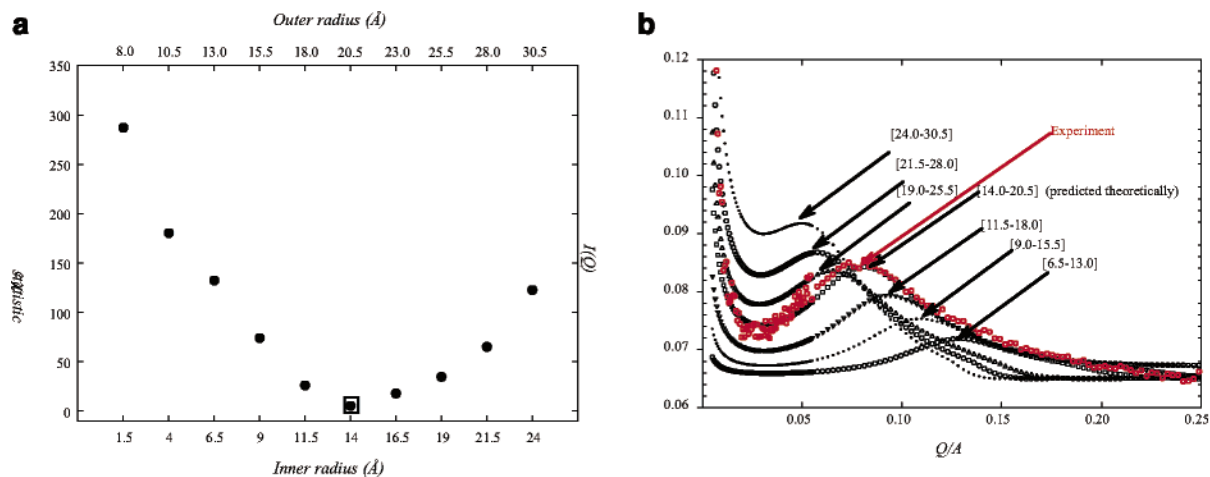
Figure 5. (a) Change in the χ^2 parameter (representing the quality of the fit) as a function of the inner radius for the 2 wt % SMA solution. The difference between the inner and outer radii was kept constant. The square represents the value of the inner and outer radii predicted theoretically. (b) Fitting curves as a function of the internal radii for the 2 wt % SMA solution. The difference between the inner and outer radii was kept constant. The values in brackets represent the inner and outer radii. The curve in red is the experimental curve of the 2 wt % SMA solution.
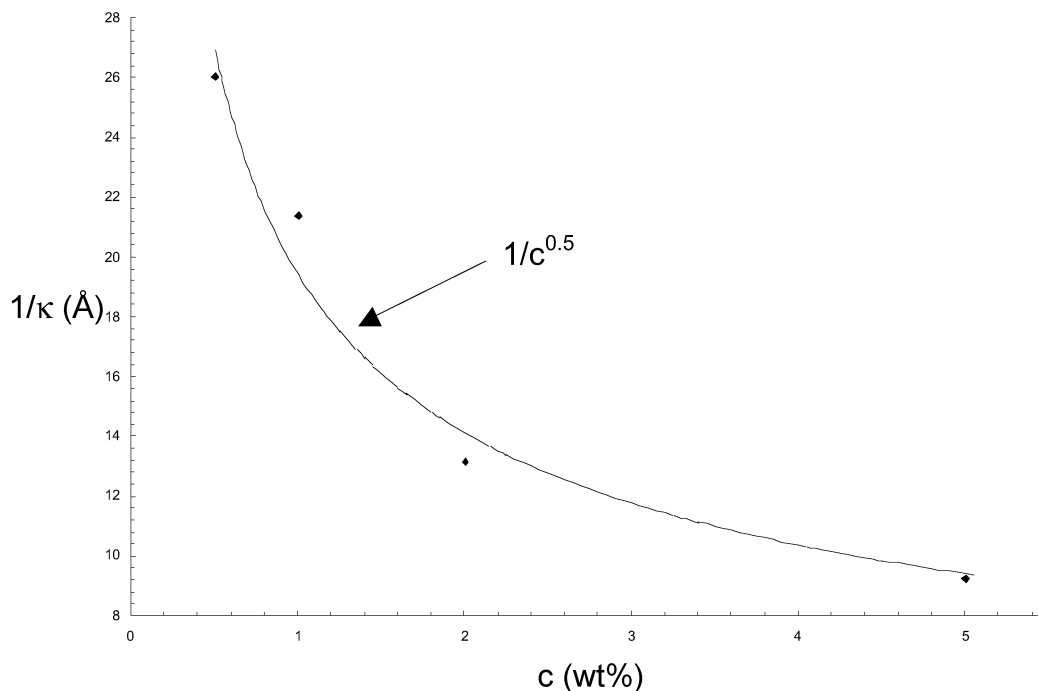
Figure 6. Best fit of Debye length as function of SMA concentration.

could also be fitted (without affecting the inner and outer diameters) by fixing $1/\kappa$ and varying A, but this is physically less realistic. Varying both parameters at the same time did not give a clear concentration dependence because these parameters are interdependent.

The effect of the increase in concentration is to shift the scattering intensity to higher values. The effect of the increase in the local volume fraction is to shift the peak to higher Q values. This observation is in good agreement with the behavior of interacting systems.[5]

Because the shift in the Q value of the peak as a function of concentration is directly related to the local volume fraction, this shift might be due to more compact structures forming as the concentration increases. The structure of the association in solution can be determined by the slope of $\log(I(Q))$ as a function of $\log(Q)$ for small Q values.[11]

Indeed, a slope of -1 corresponds to a solution containing isolated rigid rods, a slope of -2 corresponds to a solution containing sheets, and so forth. These plots were performed for the different concentrations studied and are shown in Figures 7 and 8.

The plots of $\log(I(Q))$ versus $\log(Q)$ at low Q values show two different slopes for the 0.5 and 1 wt % solutions. Note that the slopes from 2 to 10 wt % increase, suggesting that the size of the structure increases as a function of concentration. The initial slopes obtained for 0.5 and 1 wt % decrease as the second slopes increase. Taking into account only the second slope for the 0.5 and 1 wt % solutions, the slopes increase with concentration.

In addition, the absolute value of the slope for the lowest concentration is between the values expected for sheets and isolated rods, which suggests that a mixture of sheets and rods is present in solution. The presence of two slopes for 0.5 and 1 wt % may be related to two different

(11) Higgins, J.; Benoit, H. *Polymers and Neutron Scattering*; Oxford University Press: New York, 1994.
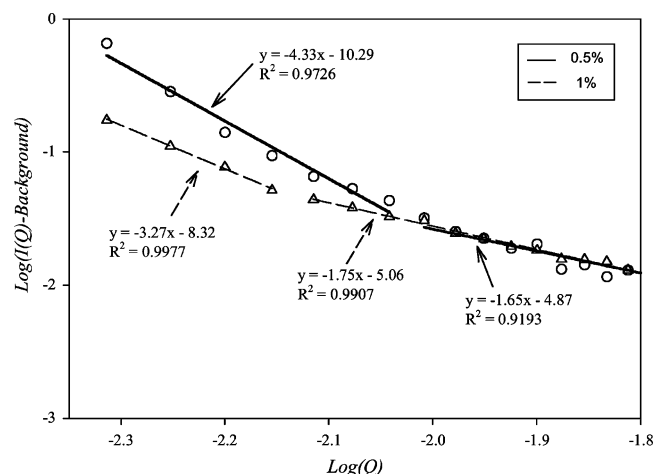
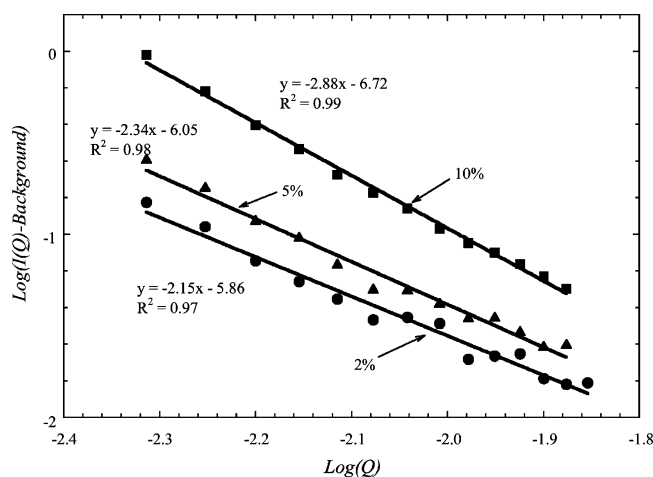**Figure 7.** $\log(I(Q))$ vs $\log(Q)$ at low Q values for 0.5 and 1 wt % solutions of SMA 40K in D_2O.

Figure 8. $\log(I(Q))$ vs $\log(Q)$ at low Q values for concentrations of SMA in D_2O at pH 7.
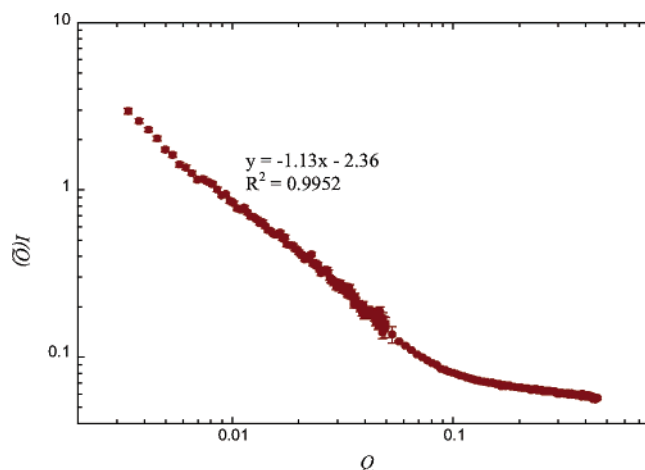

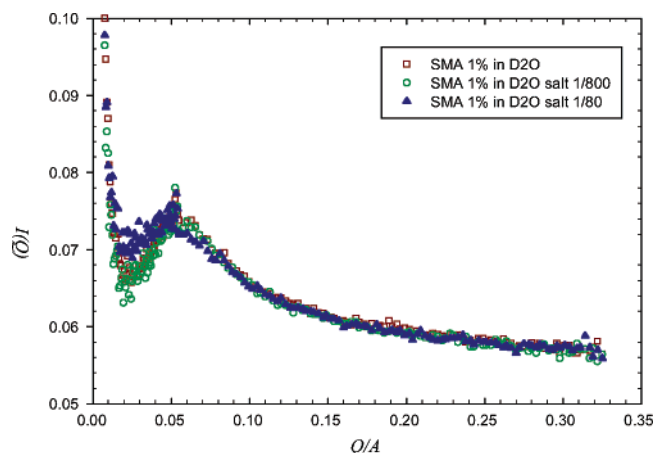**Figure 9.** Neutron-scattering profiles of a 1 wt % solution of SMA ($M_w = 1600$).

Figure 10. Neutron-scattering profiles of a 1 wt % SMA solution in D_2O for various ionic strengths ($M_w = 40\,000$).

associations of SMA molecules; the initial slope fades out as the SMA concentration increases, and a more uniform association is observed. This behavior has also been observed for single-walled carbon nanotube suspensions, and the first slope was attributed to a loose 3-D network.[12] The slope obtained for the 10 wt % solution is close to the slope expected for a 3-D object, which could correspond to the packing of sheets.

To summarize, from the changes in the scattering profile as a function of concentration, it can be concluded that as the SMA concentration increases the association becomes more compact (shift in the Q value of the peak) and the structure changes to a uniform 3-D shape (increase in the absolute value of the slope).

Molecular Weight Dependence

To characterize the molecular weight effect on the SMA association, another molecular weight SMA was studied by neutron scattering. The neutron-scattering profile of a 1 wt % SMA solution with a molecular weight of $M_w = 1600$ is shown in Figure 9.

The plot of $\log(I(Q))$ versus $\log(Q)$ at low Q values for the 1 wt % solution of SMA in D_2O corresponding to a molecular weight of 1600 has a slope of -1.13, which corresponds closely to the slope of -1 expected for isolated rods[12] (Figure 9). Because the absolute value of the slope

is greater than 1, this implies that the presence of sheets observed for the higher molecular weight is possible. The sheets were observed by a separate Cryo-TEM for a 1% solution of SMA ($M_w = 1600$).[4]

Ionic Strength Effect

The ionic strength was proven to be a dominant factor in the destabilization of various self-associated systems.[15−19] The effect of the ionic strength on the association of SMA chains was studied using three different NaCl concentrations: 0, 1/800, and 1/80 (corresponding to 0, 6 × 10^{-5}, and 6 × 10^{-4} mol/L, respectively). The fraction corresponds to the amount of salt added with respect to the amount of SMA in solution. This study was performed first on solutions of SMA $M_w = 40\,000$ (Figures 10−13) and then on solutions of SMA $M_w = 1600$ (Figures 14 and 15).

(12) Zhou, W.; Islam, M.; Wang, H.; Ho, D.; Yodh, A.; Winey, K.; Fischer, J. *Chem. Phys. Lett.* **2004**, *384*, 185.

(13) Nagarsekar, A.; Crissman, J.; Crissman, M.; Ferrari, F.; Cappello, J.; Ghandehari, H. *J. Biomed. Mater. Res.* **2002**, *62*, 195.

(14) Cosgrove, T.; White, S.; Zarbakhsh, A.; Heenan, R.; Howe, A. *J. Chem. Soc., Faraday Trans.* **1996**, *92*, 595.

(15) Pispas, S.; Hadjichristidis, N. *Langmuir* **2003**, *19*, 48.

(16) Solomatin, S.; Bronich, T.; Bargar, T.; Eisenberg, A.; Kabanov, V.; Kabanov, A. *Langmuir* **2003**, *19*, 8069.

(17) Lee, A.; Bütün, V.; Vamvakaki, M.; Armes, S.; Pople, J.; Gast, A. *Macromolecules* **2002**, *35*, 8540.

(18) Dong, X.; Gray, D. *Langmuir* **1997**, *13*, 2404.

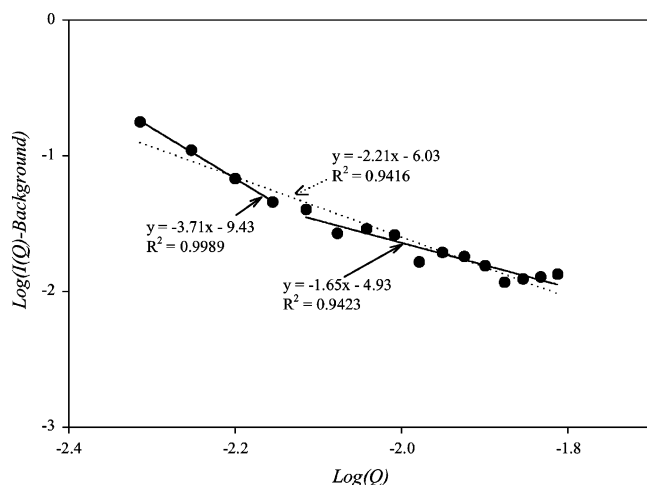(19) McAloney, R.; Sinyor, M.; Dudnik, V.; Goh, C. *Langmuir* **2001**, *17*, 6655.

Figure 11. $\log(I(Q))$ vs $\log(Q)$ at low Q values for a 1 wt % solution of SMA ($M_w = 40K$) in D_2O with an addition of salt of 1/800 shown with a linear regression using two slopes (continuous line) and one slope (dotted line).
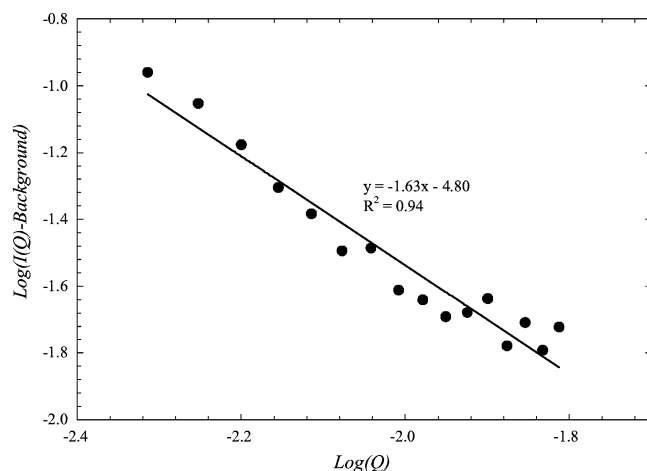

Figure 12. $\log(I(Q))$ vs $\log(Q)$ at low Q values for a 1 wt % solution of SMA ($M_w = 40K$) in D_2O with an addition of salt of 1/80.
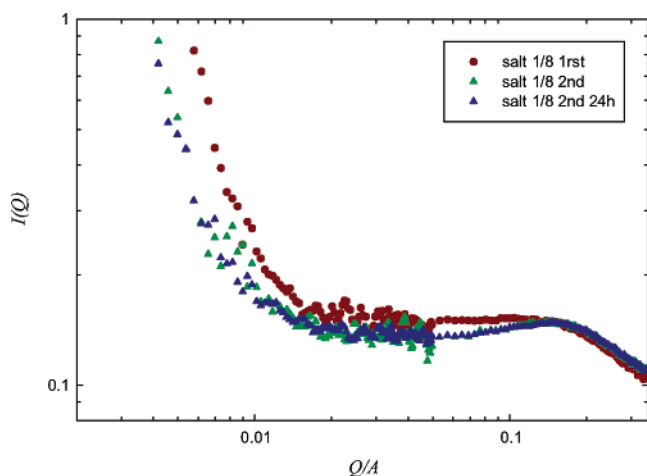

Figure 13. Neutron-scattering profiles of a 10 wt % SMA solution in D_2O at high ionic strength when the salt is added before or after SMA dissolution at pH 7.

Ionic Effect on SMA $M_w = 4000$ Solutions

The profiles obtained from the solutions with different ionic strengths are shown in Figure 10. The first addition of NaCl did not have any effect on the association because the profile with 1/800 NaCl is superimposed on that of the
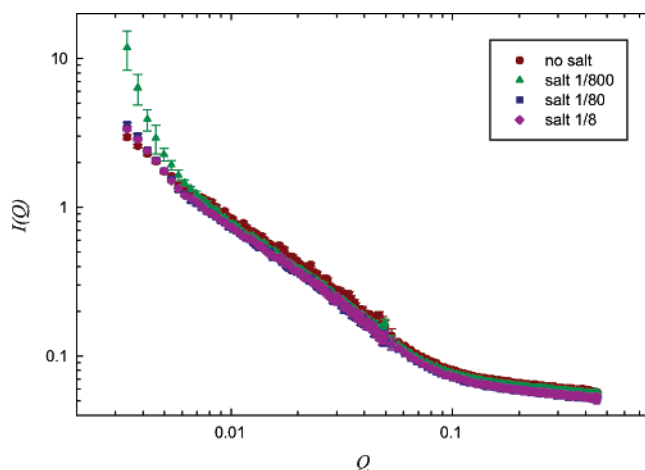

Figure 14. Neutron-scattering profiles of a 1 wt % solution of SMA ($M_w = 1600$) for various ionic strengths.
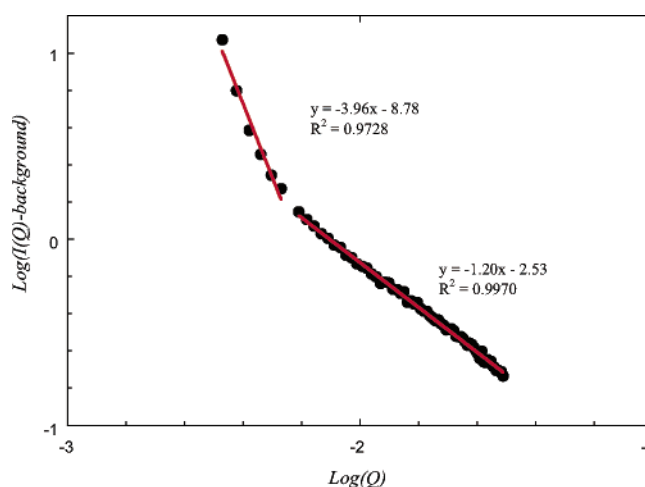

Figure 15. $\log(I(Q))$ vs $\log(Q)$ at low Q values for a 1 wt % solution of SMA ($M_w = 1600$) in D_2O with an addition of salt of 1/800.

solution containing no salt. The second addition of salt had an effect on the association, as a shift was observed in the peak of the scattering profile (Figure 10). The peak was shifted to lower Q values and corresponds to a less compact structure observed when the concentration of SMA decreases.

The plot of $\log(I(Q))$ as a function of $\log(Q)$ at low Q values for the 1 wt % solution with 1/800 NaCl did not reveal an increase in the absolute value of the slope from the value obtained for the second slope of the 1 wt % solution without salt (Figure 11).

Furthermore, the plot of $\log(I(Q))$ versus $\log(Q)$ at low Q values for the 1 wt % solution with 1/80 of NaCl shows a decrease in the absolute value of the slope from the value obtained for the slope of the 1 wt % solution with 1/800 of NaCl. Thus, the addition of a larger amount of salt disrupts the SMA association, and the size of the structure decreases. The plot of $\log(I(Q))$ versus $\log(Q)$ at low Q values for the 1 wt % solution with 1/80 NaCl is shown in Figure 12.

The ionic strength effect was also studied with a 10 wt % solution of SMA. Indeed, it was proven that a more compact structure was formed for a high-concentration solution. Therefore, this structure might be less affected by the presence of salt. To study this effect, two solutions were prepared. In the first one, the salt (NaCl) was added to a $D_2O/NaOH$ solution, and then SMA was dissolved in this solution. In the second preparation, SMA was

Table 3. Two Different Matches Used to Determine the Hydrophilic and Hydrophobic Interactions within the SMA Association[a]

	Styrene D₈	*Maleic acid*
SLD (*10⁻⁵Å⁻²)	0.560	0.288
Match (D₂O:H₂O)	m_D(9:1)	m_H(5:5)
Visible Part	Hydrophilic	Hydrophobic

[a] The visible part of each match is in dark gray.

dissolved in the D_2O/NaOH solution, and the salt (NaCl) was added 15 min prior to the experiment. Two scattering profiles were taken for the second solution to ensure that the scattering profile obtained was at equilibrium.

The main difference between the profiles of the two solutions lies in the disappearance of the peak for the first solution (Figure 13), which was observed without salt for the 10 wt % solution (Figure 4). When the salt is added to the SMA solution, the same peak is observed. Therefore, the structure obtained at high ionic strength is different when the salt is added after or before the compact tubular structure is formed. The profile obtained for the second solution (when the salt is added prior the experiment) is stable as the profile obtained for this solution after 24 h is stable (Figure 13).

Ionic Effect on SMA M_w = 1600 Solutions

The solution of SMA (M_w = 1600) shows a very strong dependence on the ionic strength (Figure 14). Indeed, a very small addition of salt gives rise to a large increase in scattering intensity at low Q values (Figure 14). As more salt is added to the solution, the slope decreases to its original value corresponding to isolated rods.

The increase in intensity observed at low Q values with a very small addition of salt to the 1 wt % solution (M_w = 1600) is revealed by the plot of $\log(I(Q))$ versus $\log(Q)$ at low Q values (Figure 15). This plot shows two different slopes—one close to the value expected for isolated rods and the other close to the value expected for a 3-D object. This large increase in size was also observed by light scattering,[20] this technique being very sensitive to large structures.

Hydrophilic and Hydrophobic Structure

To characterize the structure of the hydrophilic and hydrophobic parts of SMA, a deuterated polymer was used. The labeling of the polymer was performed on the styrene part of SMA. As explained previously, the scattered intensity is dependent on the contrast between the solvent and the polymer studied. Consequently, if the SLD of the solvent matches the styrene part of SMA (the deuterated part) then the SLD contrast will be due to the difference between the hydrophilic part of SMA and the solvent–styrene part. Using this match, the contribution of the hydrophobic part of SMA will be erased from the scattering curve, and only the hydrophilic contribution will be observed.

Using the labeling method, two matches were used. The first one, the m_D match, is a match on the deuterated part of SMA, and the second match, m_H, is a match on the hydrogenated part of SMA. Consequently, the first match
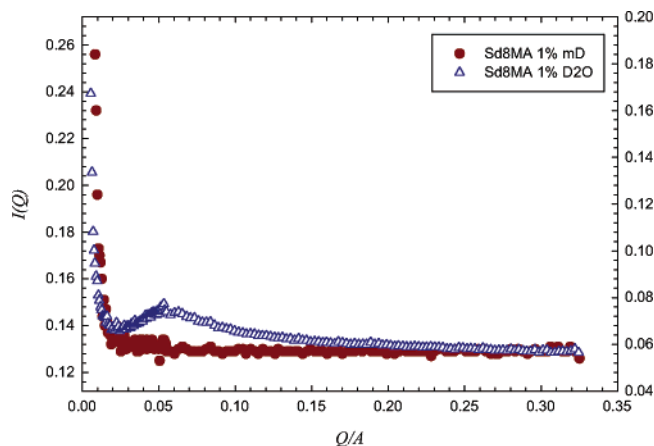
(20) Vyhnalkova, R. Internal Report; McGill University, 2000.

Figure 16. Neutron-scattering profiles of a 1 wt % SMA solution in m_D (circles) and in D_2O (triangles). The m_D profile represents the contribution of the hydrophilic part of SMA in the association.
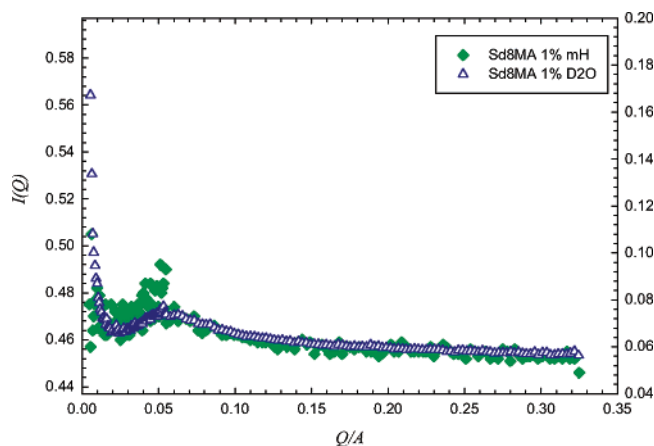

Figure 17. Neutron-scattering profiles of a 1 wt % SMA solution in m_H (diamonds) and in D_2O (triangles). The m_H profile represents the contribution of the hydrophobic part of SMA in the association.

shows the structure of the hydrophilic part of SMA, and the second shows the structure of the hydrophobic part of SMA.

The two different matches as well as the SLD of the hydrophilic and hydrophobic parts of SMA are listed in Table 3. The two drawings in Table 3 show in dark gray the visible part of SMA during the m_H and m_D experiments. The m_H and m_D scattering curves are in Figures 16 and 17, respectively.

Figure 16 shows the overlay of the Sd_8MA curves obtained in D_2O and the m_D mixture of D_2O and H_2O. In this Figure, no peak was observed in the scattering curve,
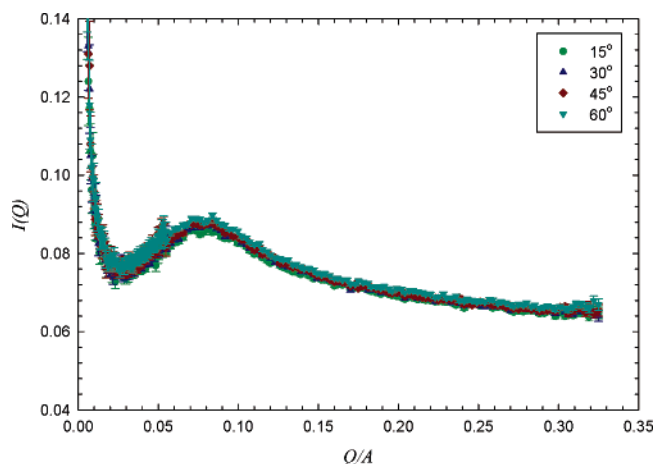
Figure 18. Neutron-scattering profiles of 2 wt % SMA solutions at pH 7 for various temperatures.

Figure 19. Neutron-scattering profiles of a 1 wt % solution of SMA at pH 12 (M_w = 40K) (circles) and the corresponding fit (line).

and this might indicate that no direct interaction occurs between the hydrophilic parts of SMA. However, the same increase at low Q values was present in the profile.

Figure 17 shows the overlay of the Sd_8MA curves obtained in D_2O and m_H mixture of D_2O and H_2O. In this Figure, the peak observed for Sd_8MA in D_2O at $Q \approx 0.06$ $Å^{-1}$ is still present when we observe the hydrophobic part of SMA, which confirms the hydrophobic origin of the self-association between the SMA chains at pH 7. The structure observed for SMA at pH 7 can therefore be associated with the structure of the hydrophobic interactions. The increase at low Q values is also observed in Figure 17.

Thermal Stability

Thermodynamics is a very important concept for the stability of self-assembled systems. Previous SANS studies of self-assembled block copolymers have shown that the size of the aggregates can be increased or decreased as a function of temperature.[13−15] For biological systems, these interactions are also very important and determine the stability of the receptor−ligand interactions.

In this study, the thermal stability was investigated using a controlled temperature bath around the sample holder of the SMA solution. A 2 wt % solution in D_2O was chosen as an intermediate value of the concentration range studied previously. A temperature range of 15−75 °C was used for the thermal stability study of the association by an increase of 15 °C between each run, and the scattering curves obtained are shown in Figure 18. To control the temperature of the scattering cells, the sample holders were immersed in a temperature-controlled bath. Because the volume of each cell is very small (1 mL), 10 min was allowed for the solution to equilibrate before starting the experiment.

The large change in temperature does not affect the stability or the shape of the association. Indeed, the four scattering curves shown in Figure 18 are almost identical. This thermal stability of the system shows that the entropy term is negligible compared to the enthalpy term and confirms the theoretical prediction of the origin of the association between the SMA chains.[4] Indeed, the change in entropy between two noninteracting chains of SMA at pH 7 and two associated chains is very small compared to the stabilization due to the enthalpy of association. The entropy term remains small for all temperatures studied.

pH Dependence

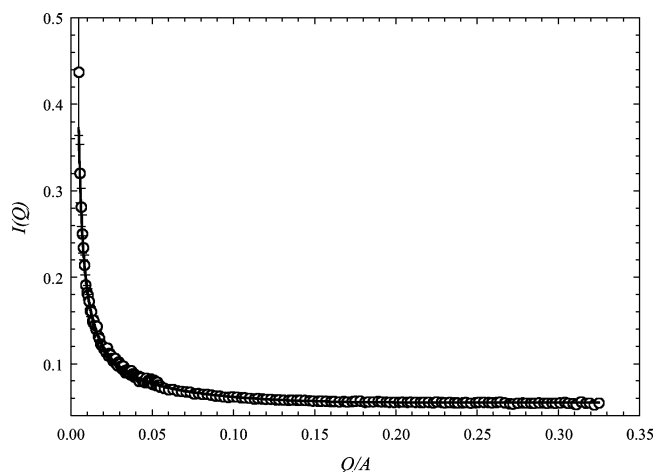The theoretical calculations and the experimental characterization of the SMA association have shown that

the structure obtained is very dependent on pH. Because it is very difficult to solubilize SMA at low pH, only a scattering profile of SMA at a high pH value was obtained and is shown in Figure 19. This profile has a monotonic decay, showing no structure. The profile was fitted using a Pederson worms model,[21−23] and the fit is also shown in Figure 19 (continuous line). As a starting point for the optimization of the parameters, the known scattering-length density between the solvent and the solute and volume fraction of the solute were used.

In this model, the chains are considered to be semi-flexible, and three main parameters are determined: the contour length of the structure, the Kuhn length (which gives the flexibility of the structure), and the cross-sectional radius. If the SMA chain (corresponding to a molecular weight of 40K) had been completely linear, then the corresponding contour length would have been about 240 nm. The contour length obtained from the fitting is in fact 146 nm, which indicates that the structure is not completely linear. However, the Kuhn length obtained is very large, 82 nm, which indicates that the structure is very rigid. In addition, the cross-sectional radius of a completely linear SMA chain would be about 5.4 Å whereas the cross-sectional radius obtained by this method is 16.3 Å. Therefore, different chain shapes obtained by the theoretical results[3] might explain the difference in the cross-sectional radius from a linear chain, and the small contour length obtained compared to those of a linear chain.

Ethyl Ester of SMA

To complete the investigation of the association of SMA chains in water at pH 7, a derivative of SMA was studied: the ethyl ester of SMA. The profile of the 1 wt % EE−SMA solution in D_2O at pH 7 is shown in Figure 20. This profile is very similar to the 1 wt % SMA profile, as indeed the same increase at low Q values is observed. In addition, the peak observed for the 1 wt % SMA solution is also observed in this profile at the same Q value. The main difference between the two profiles is the intensity of the peak, which is more pronounced in the EE−SMA profile. To explain this structural difference, a complete theoretical study of EE−SMA is needed.

(21) Pedersen, J.; Schurtenberger, P. *Macromolecules* **1996**, *29*, 7602.
(22) Pedersen, J. *J. Appl. Cryst*. **2000**, *33*, 637.
(23) Arleth, L.; Bauer, R.; Ogendal, L.; Egelhaaf, S.; Schurtenberger, P.; Pedersen, J. *Langmuir* **2003**, *19*, 4096.
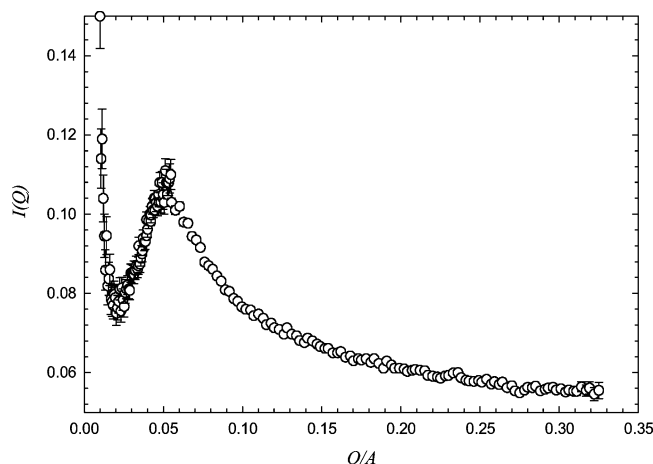
Figure 20. Neutron-scattering profiles of a 1 wt % solution of EE−SMA at pH 7 (M_w = 40K) in D_2O.

Conclusions

In this article, an extensive study of the SMA chain association is presented, using neutron-scattering results. The fitting of the neutron-scattering profiles has confirmed the tubular structure of the association as well as the size obtained by theoretical calculations. The tubular structure has inner and outer radii experimentally determined to be about 13 and 21 Å, respectively.

In addition, the effect of the concentration on the SMA association shows that SMA forms a more compact structure as the concentration increases, as the local volume fraction of the association increases with concentration.

The molecular weight dependence investigation has shown that the association of low molecular weight SMA consists mainly of individual tubes. However, a high molecular weight polymer will form higher-order structures.

To study the stability of the association, two factors were varied: the temperature and the ionic strength. The association has shown no dependence on temperature. Indeed, the scattering profiles obtained for temperatures varying between 15 and 75 °C were superimposed. The study of the ionic strength dependence has revealed that the addition of a very small amount of salt to the solution increases the size of the association. However, when more salt is added to the solution, the size of the association decreases, and the structure is altered. This effect is very strong when the salt (NaCl) is added before the tubular structure is formed, but for a high-concentration SMA solution, the structure is compact and the ionic effect is not very strong when the salt is added after the formation of the association.

Furthermore, the study of SMA solutions at pH 12 has shown that the polymer has a wormlike rigid conformation. No association between the chains was observed from the neutron-scattering profile at this pH.

LA050888A